

OPEN ACCESS

EDITED BY

Muhammad Wasim, University of Florence, Italy

REVIEWED BY

Shivani R Pandya,

Narnarayan Shastri Institute of Technology,

India Ganesh Yadagiri,

The Ohio State University, United States

*CORRESPONDENCE

RECEIVED 19 February 2025 ACCEPTED 04 August 2025 PUBLISHED 09 September 2025

CITATION

Alvizo-Báez CA, de Jesús González-Escobedo M, Terrazas-Armendáriz LD, Uscanga-Palomeque AC, Luna-Cruz IE, Martínez-Ruíz AM, Ruíz-Robles MA, Pérez-Tijerina EG, Tamez-Guerra R, Rodríguez-Padilla C and Alcocer-González JM (2025) Quercetin self-assembly nanoparticles with antiviral molecules are effective in inhibiting SARS-CoV-2 pseudovirus infection. Front. Nanotechnol. 7:1579997. doi: 10.3389/fnano.2025.1579997

COPYRIGHT

© 2025 Alvizo-Báez, de Jesús González-Escobedo, Terrazas-Armendáriz, Uscanga-Palomeque, Luna-Cruz, Martínez-Ruíz, Ruíz-Robles, Pérez-Tijerina, Tamez-Guerra, Rodríguez-Padilla and Alcocer-González. This is an open-access article distributed under the terms of the Creative Commons Attribution License (CC BY). The use, distribution or reproduction in other forums is permitted, provided the original author(s) and the copyright owner(s) are credited and that the original publication in this journal is cited, in accordance with accepted academic practice. No use, distribution or reproduction is permitted which does not comply with these terms

Quercetin self-assembly nanoparticles with antiviral molecules are effective in inhibiting SARS-CoV-2 pseudovirus infection

Cynthia Aracely Alvizo-Báez¹,
Marlon de Jesús González-Escobedo¹,
Luis Daniel Terrazas-Armendáriz¹,
Ashanti Concepción Uscanga-Palomeque¹,
Itza Eloisa Luna-Cruz¹, Amalia Maricela Martínez-Ruíz¹,
Mitchel Abraham Ruíz-Robles², Eduardo Gerardo Pérez-Tijerina²,
Reyes Tamez-Guerra¹, Cristina Rodríguez-Padilla¹ and
Juan Manuel Alcocer-González¹*

¹Laboratorio de Inmunologia y Virololgía, Facultad de Ciencias Biológicas, Universidad Autónoma de Nuevo León, San Nicolás de Los Garza, NL, México, ²Centro de Investigación en Ciencias Físico Matemáticas, Facultad de Ciencias Físico Matemáticas, Universidad Autónoma de Nuevo León, Ciudad Universitaria, San Nicolás de los Garza, NL, México

Polyphenols have recently attracted considerable interest in the development of nanotechnological antiviral strategies. Among them, quercetin is a natural compound with strong antioxidant activity, exceeding that of vitamins C and E, and notable anti-inflammatory properties in respiratory diseases. In this study, quercetin nanoparticles (QCT-NPs) were synthesized and conjugated with remdesivir, an FDA-approved antiviral drug, or curcumin, a natural molecule with well-documented antiviral effects. The antiviral activity of these conjugates was evaluated through pseudovirus neutralization assays using Vero E6 cells, which provide a reliable model due to their high expression of SARS-CoV-2 receptors. The results demonstrated that QCT-NPs + Rem achieved 72.7% neutralization, while QCT-NPs + Cur reached 79.8% against the alpha variant. Notably, both formulations showed improved activity against the delta variant, with QCT-NPs + Rem achieving 98% neutralization and QCT-NPs + Cur 88%. These findings reveal the significant enhancement of antiviral activity when quercetin nanoparticles are conjugated with either remdesivir or curcumin, compared with the effects of the free molecules. Overall, the study highlights the potential of polyphenol-based nanocarrier systems as promising therapeutic strategies against SARS-CoV-2 variants. Further in vivo validation and clinical studies are warranted to explore their translational applications.

KEYWORDS

remdesivir, curcumin, quercetin nanoparticles, drug delivery, nanocarriers

1 Introduction

Technological advancements have significantly contributed to the control and, in some cases, eradication of life-threatening viral diseases such as smallpox and poliomyelitis (Zhou et al., 2021). However, the dynamic nature of the modern world, characterized by increased globalization, ecological disruption, and climate change, continues to facilitate the emergence of novel viral pathogens and the evolution of existing ones. These factors heighten the risk of new epidemics and pandemics, as exemplified by the recent global outbreak of coronavirus disease 2019 (COVID-19) caused by severe acute respiratory syndrome coronavirus 2 (SARS-CoV-2) (Baker et al., 2022).

SARS-CoV-2 infection presents a wide clinical spectrum, ranging from asymptomatic cases or mild respiratory symptoms to severe pneumonia, acute respiratory distress syndrome (ARDS), multiorgan failure, and death (Wu and McGoogan, 2020). The estimated evolutionary rate of SARS-CoV-2 ranges from 0.0004 to 0.002 nucleotide substitutions per site per year, indicating moderate genetic plasticity. On 31 May 2021, the World Health Organization (WHO) implemented a Greek-letter naming system for variants of concern (VOCs), categorizing them as Alpha (B.1.1.7), Beta (B.1.351), Gamma (P.1), and Delta (B.1.617) (Tao et al., 2021).

The rapid global spread of SARS-CoV-2 highlighted the urgent need for effective therapeutic interventions. In response, multiple strategies were pursued, including antiviral agents targeting viral entry and replication, immunomodulatory therapies to mitigate the cytokine storm, convalescent plasma therapy, and the unprecedented acceleration of vaccine development (Pascual-Figal et al., 2022; Doi et al., 2021). However, the continuous emergence of viral variants has posed significant challenges to the long-term efficacy of vaccines, necessitating ongoing adaptation and the development of novel therapeutic approaches (Lipsitch and y Eval, 2017; Ulmer et al., 2006). Among these, the repositioning of existing drugs has emerged as a pragmatic strategy. In particular, naturally derived compounds such as quercetin and curcumin, previously reported to exhibit antiviral activity against pathogens like the influenza virus, are being investigated for their potential inhibitory effects against SARS-CoV-2 (Derosa et al., 2021).

However, optimizing drug delivery remains a significant challenge in ensuring therapeutic efficacy, minimizing systemic toxicity, and preventing the development of drug resistance. In this context, the integration of advanced drug delivery systems, particularly nanocarriers, offers a promising strategy for enhancing pharmacokinetic profiles, improving target specificity, and enabling the controlled release of antiviral agents (Jackman et al., 2016).

The hydrophobicity of the quercetin molecule is a key factor in forming water-soluble quercetin nanoparticles. This property allows the encapsulation of biologically relevant molecules and particles, offering protection against oxidation, isomerization, and degradation, which helps extend their half-life. These encapsulated quercetin nanoparticles can be used for controlled and sustained delivery (Chiu et al., 2007). Additionally, encapsulation enhances the solubility of hydrophobic molecules and particles, thereby improving their mechanism of action within target cells and tissues. This method is especially useful for the targeted delivery of genes and therapeutic agents that may be cytotoxic. As a result, nanoencapsulation greatly boosts bioavailability and reduces toxicity (Bernardy et al., 2010).

In the current study, we standardized a method for constructing bifunctional nanocarriers using the polyphenol quercetin based on the methodology of Kumari A et al. (2010) and Chiu et al. (2007). This method involved encapsulating antiviral drugs such as curcumin and remdesivir, both known for their anti-inflammatory and antioxidant properties. The main goal was to evaluate their antiviral activity and to determine whether these nanocarriers could improve the efficacy of remdesivir and curcumin against the SARS-CoV-2 pseudovirus.

2 Materials and methods

2.1 Synthesis of quercetin nanoparticles (QCT-NPs)

Quercetin nanoparticles were synthesized through oxidative self-polymerization in alkaline conditions. Inspired by the methodology described by Sunoqrot et al. (2019), 10 mg of quercetin hydrate (Cayman Chemicals, 10005169—concentration 3×10^{-5} M), was first dissolved in 1 mL of 99% DMSO, then we immediately added 7 mg of NaIO4 (Sigma Aldrich—concentration 4×10^{-5} M). It was mixed until a homogeneous solution was obtained and kept under constant agitation (12,000 rpm) at room temperature for approximately 12 h. It was thence passed through a porous molecular membrane (MWCO 3.5 kDa, 29 nm diameter) and placed in a flask with 200 mL of deionized water and 165 mg of buffer bicine (Sigma Aldrich—concentration 0.06 M) and kept under agitation at 300 rpm.

The water was changed every hour under the same conditions for the first 4 h; after that, it was left for 24 h. Subsequently, it was centrifuged at 7,000 rpm for 10 min, the supernatant was taken, and it was centrifuged again at 12,000 rpm for 10 min. The supernatant was then removed without disturbing the sediment, resuspended, and stored for stability tests at room temperature (TR), 4 $^{\circ}$ C, and -20 $^{\circ}$ C.

The construction of quercetin nanocomplexes with remdesivir and curcumin is based on the IC50 values of the components. A concentration of 18.20 μM of quercetin (Kandeil et al., 2021) was dissolved in 200 μL of DMSO and stirred at 700 rpm for 3 h at 60 °C (Sunoqrot et al., 2019; Oliver et al., 2017). Following the methodology of Sunoqrot et al. (2019), the solution was allowed to cool, and 20 μM of mPEG5K-NH2 was added. The mixture was kept under constant stirring for 12–18 h. Subsequently, either 0.987 μM of remdesivir (Pizzorno et al., 2020) or 0.0448 μM of curcumin (Kandeil et al., 2021) was added and stirred for an additional 24 h. Finally, the solution was passed through a porous membrane, and dialysis was performed under the same conditions described earlier. For stability tests, the nanocomplexes were stored at RT, 4 °C, and –20 °C for 6 weeks.

2.2 Synthesis of quercetin nanoparticles with remdesivir (QCT-NPs + Rem) and quercetin nanoparticles with curcumin (QCT-NPs + Cur)

2.2.1 Formation of guercetin oligomers

Quercetin was dissolved in DMSO and stirred at 700 rpm for 3 h at 60 °C (Sunoqrot et al., 2019; Oliver et al., 2017). After cooling,

 $20\,\mu\text{M}$ of mPEG5K-NH2 was added, and the mixture was kept under constant agitation for 12–18 h. Subsequently, remdesivir or curcumin was added (Pizzorno et al., 2020). Finally, the solution was transferred to a porous molecular membrane, and dialysis was performed under the same conditions described above.

2.3 Characterization of QCT-NPs, QCT-NPs + Rem, and QCT-NPs-Cur

2.3.1 Size by dynamic light scattering

The distribution of the size of the particles by DLS was determined by means of a Malvern Zetasizer ZS90 using 12-nm polyethylene cells, taking the analyzed samples to a 1:100 dilution. All readings were done in triplicate.

2.3.2 Shape and size by atomic force microscopy

To prepare the samples for the AFM, they were taken to 1:100 or 1:1000 dilution, and a drop was added to a mica glass and was allowed to dry in the environment. Subsequently, it was analyzed in the equipment (FEI Quanta 250).

2.3.3 Zeta potential

The zeta potential of the nanoparticles was measured in the Malvern Zetasizer ZS90, diluting the samples in FBS serum to a concentration of 1:100 or 1:1000 using disposable folded capillary cells (Malvern). All readings were done in triplicate.

2.3.4 UV absorbance spectra

Samples $50 \,\mu\text{L/well}$ were analyzed on the Varioskan Lux over an approximately $200\text{--}500 \,\text{nm}$ absorbance spectrum.

2.3.5 Efficiency of encapsulation and drug release of QCT-NPs

The percentage of encapsulation efficiency was obtained through the protocol of Nathiya et al., 2014 using the formula:

%EE = [(Drug added - Free "unentrapped drug")/Drug added]*100

After synthesis, they were centrifuged at 13,500 rpm for 15 min, and then the supernatant was taken and measured in the Varioskan LUX at the wavelength of the drug to be analyzed.

The release of the drugs (Rem and Cur) was determined by obtaining 500 μL of the sample in an Eppendorf tube up to 1 mL with PBS and 10% of ethanol (Nathiya, et al., 2014), incubated in a thermomixer with 450 rpm shaking at 37 °C for 30 min, and then centrifuged at 13,500 rpm to recover the supernatant, which was read at 254 and 420 nm. Measurements were made every hour.

2.4 *In vitro* evaluation of (QCT-NPs, QCT-NPs-Rem and QCT-NPs-Cur)

2.4.1 Cell culture Vero E6

The cell culture Vero E6 comes from the African green monkey kidney, obtained from the American Type Culture Collection (ATCC crl-1586). The culture in Dulbecco's modified Eagle medium (DMEM) (Thermo Fisher Scientific) was supplemented

with 10% FBS and 1% antibiotic/antifungal (A/A) at 37 $^{\circ}$ C in 5% CO₂ for 3–5 days until the confluence reached 80%.

2.4.2 Viability assay of nanoparticles

Viability was assessed using the protocol proposed by Uliasz and Hewett (2000). A total of 8 \times 104 Vero E6 cells were added to each well of a 24-well plate and supplemented with 500 μL DMEM, 10% FBS, and 1% AA. The cells were incubated for 6 h at 37 $^{\circ} C$ in a 5% CO $_2$ atmosphere until adherence was observed. After the incubation period, the cells were examined under an immersion microscope (VWR International). Nanoparticles or free drugs were added in triplicate, resuspended in the medium, and allowed to grow under the aforementioned conditions for 48 h.

We added 21.43 μ L of filtered 0.4% trypan blue to assess the cell viability. The plates were incubated for 15 min at 37 °C. Subsequently, the medium was removed, and four washes were performed with cold PBS 1X (pH 7.4). Cell lysis was achieved by adding 1 mL of 1% SDS to each well, using a micropipette to induce mechanical disruption. Finally, the absorbance was measured at 590 nm using the Varioskan LUX. The viability standardization was calculated by determining the average absorbance of the wells in triplicate and comparing it to the positive control, which consisted of cells in wells treated with biological-grade ethanol, known to induce approximately 100% cell death. The following equation was employed to determine the percentage of viability. The data were plotted in GraphPad Prism (GraphPad Inc.) to observe the mean and standard deviation (SD).

2.4.3 Neutralization assay of pseudovirus

To determine the neutralization of the SARS-CoV-2 pseudovirus (rSARS-CoV-2), 2 \times 104 Vero E6 cells (ATCC CRL-1586) were seeded in 96-well plates containing 100 μL of DMEM supplemented with 10% FBS and 1% AA. The cells were incubated at 37 °C in a 5% CO2 for 6 h until they reached 80% confluence and demonstrated immediate adherence. For the Wuhan pseudovirus, 5 μL of rSARS-CoV-2 Spike-in Pseudotyped Luciferase, purchased from Creative Diagnostics (Shirley, NY, USA; Product No: COV-PS01, Lot: CL-114A), was added. For the Delta variant, 30 μL of COVID-19 (BioSource n.d.) was used.

The corresponding treatments were added in triplicate based on the IC50 value. The samples were then incubated for 48 h at 37 °C with 5% CO₂. After the incubation period, the medium was carefully removed without disturbing the bottom of the well. For the Wuhan variant, $50\,\mu\text{L}$ of Cell Culture Lysis 5X Reagent (Promega) was added to each well, followed by incubation for 15 min at 37 °C to ensure proper cell lysis. After this step, the mixture was transferred to a white 96-well plate with a transparent bottom (Costar Corning), and 100 µL of renilla luciferase (Promega) was added for immediate luminescence analysis using the Varioskan LUX. For the Delta variant, 100 µL of the One Glo Luciferase Assay System was added, and the samples were incubated for 30 min in the dark at 37 °C before luminescence analysis with the Varioskan LUX. The percentage of neutralization was calculated using the analyzed RLUs, with untreated wells serving as the positive control (RLU control). The calculation was performed using following formula:

Neutralization (%) =
$$\left(1 - \frac{\text{RLU}_{\text{treated}}}{\text{RLU}_{\text{control}}}\right) \times 100$$

2.5 Statistical analysis

A one-way and two-way ANOVA test were performed for multiple comparisons of means using the Tukey test. Tests and data graphs were performed using GraphPad statistical software.

3 Results

3.1 Characterization of QCT-NPs, QCT-NPs-Rem, and QCT-NPs-Cur

3.1.1 QCT-NPs

3.1.2 QCT-NPs-rem

3.1.3 QCT-NPs-cur

3.1.4 Stability of NPs

The QCT-NPs exhibited homogeneity with an average size of 209 nm (Figure 1A) and a zeta potential of –34.7 mV, characterized by a maximum peak of –34.7 mV at 100% intensity and a standard deviation of 5.78 mV. Additionally, the conductivity was measured at 0.0113 m/cm, indicating good reading quality (Figure 1B). The morphology of the QCT-NPs observed through atomic force microscopy (AFM) revealed a spherical shape with a size of approximately 200 nm (Figure 1C).

The QCT-NPs-Rem exhibited a homogeneous size distribution with an average diameter of 199.2 nm (Figure 2A), a zeta potential of -25.0 mV, and good conductivity measured at 0.0338 m/cm (Figure 2B).

The QCT-NPs-Cur exhibited a homogeneous size distribution with an average diameter of 214.6 nm (Figure 3A), a zeta potential of −19.0 mV, a conductivity of 0.0189 m/cm, and demonstrated

good quality in measurements (Figure 3B). A resume of physicochemical parameters is in Table 1.

After 30 days, the nanoparticles were stored at RT, 4 °C, and -20 °C to evaluate their stability (Table 2). The samples maintained at RT exhibited reduced stability, with QCT-NPs experiencing a substantial decrease in size. The variation in the sizes of the nanoparticles at RT indicates a lack of uniformity. Statistical analysis revealed a significant increase or decrease (p < 0.001) in the samples treated at RT compared to those stored at 4 °C and -20 °C, which remained stable. No significant differences were observed between the latter two storage conditions.

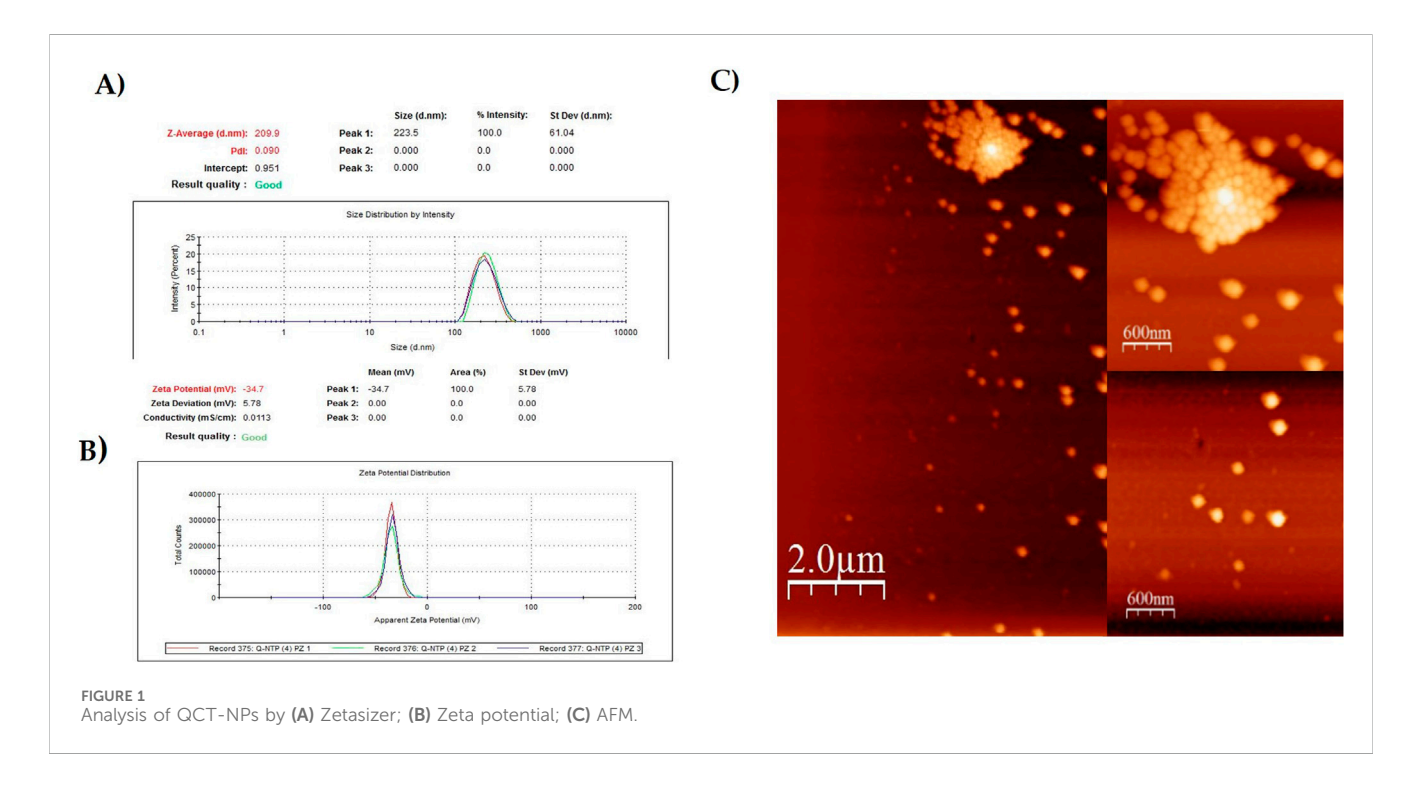
3.1.5 UV absorbance spectra

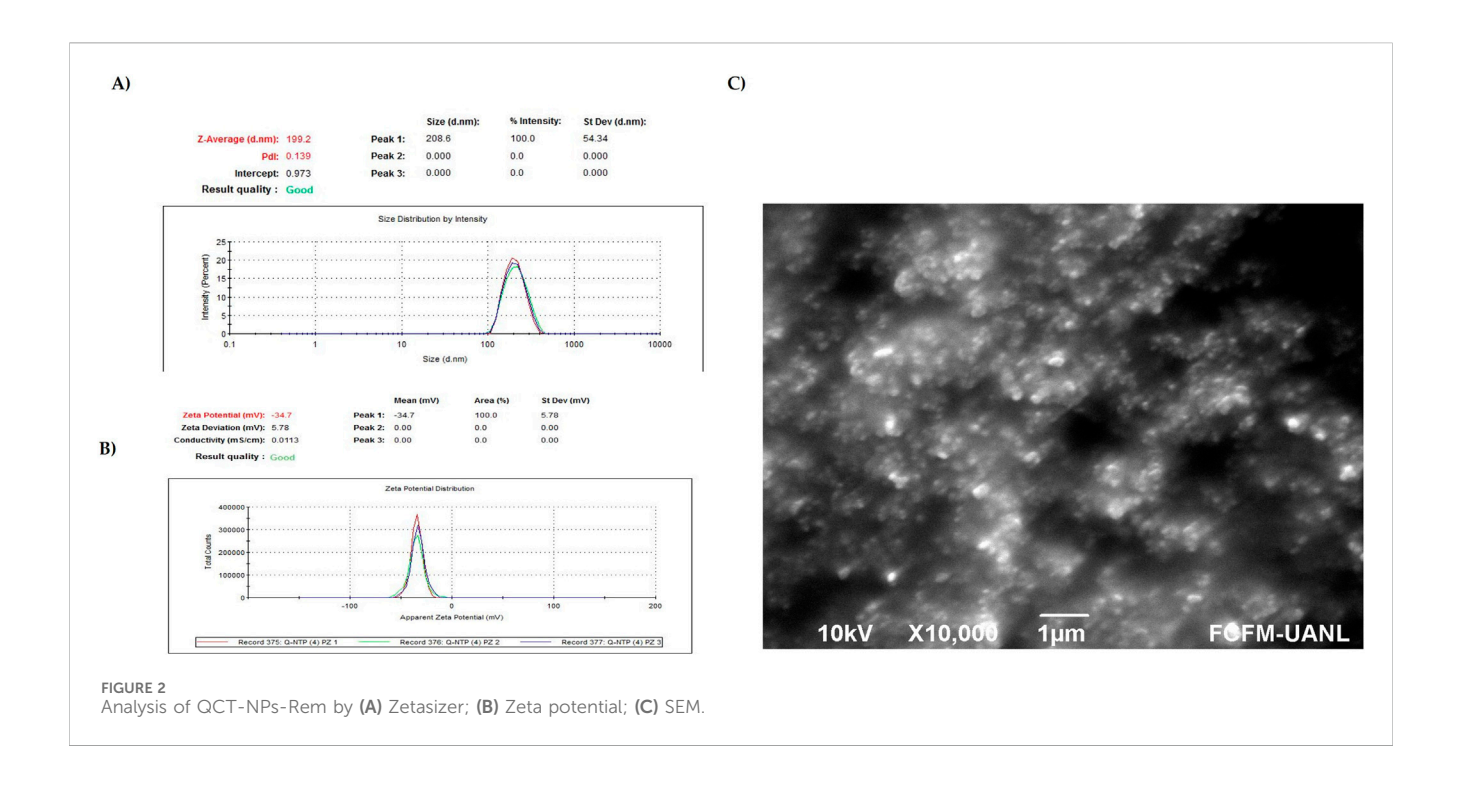
Figure 4 presents the UV–Vis absorption spectra of the quercetin-based nanoparticles (QCT-NPs). A characteristic absorption peak is observed in the range of 300–340 nm, which corresponds to quercetin. Additionally, the spectra of the drug-loaded formulations exhibit distinct absorption bands associated with their respective drugs: QCT-NPs + Rem displays an additional peak between 240 and 270 nm, attributed to remdesivir, while QCT-NPs + Cur shows a peak within the 400–480 nm range, characteristic of curcumin.

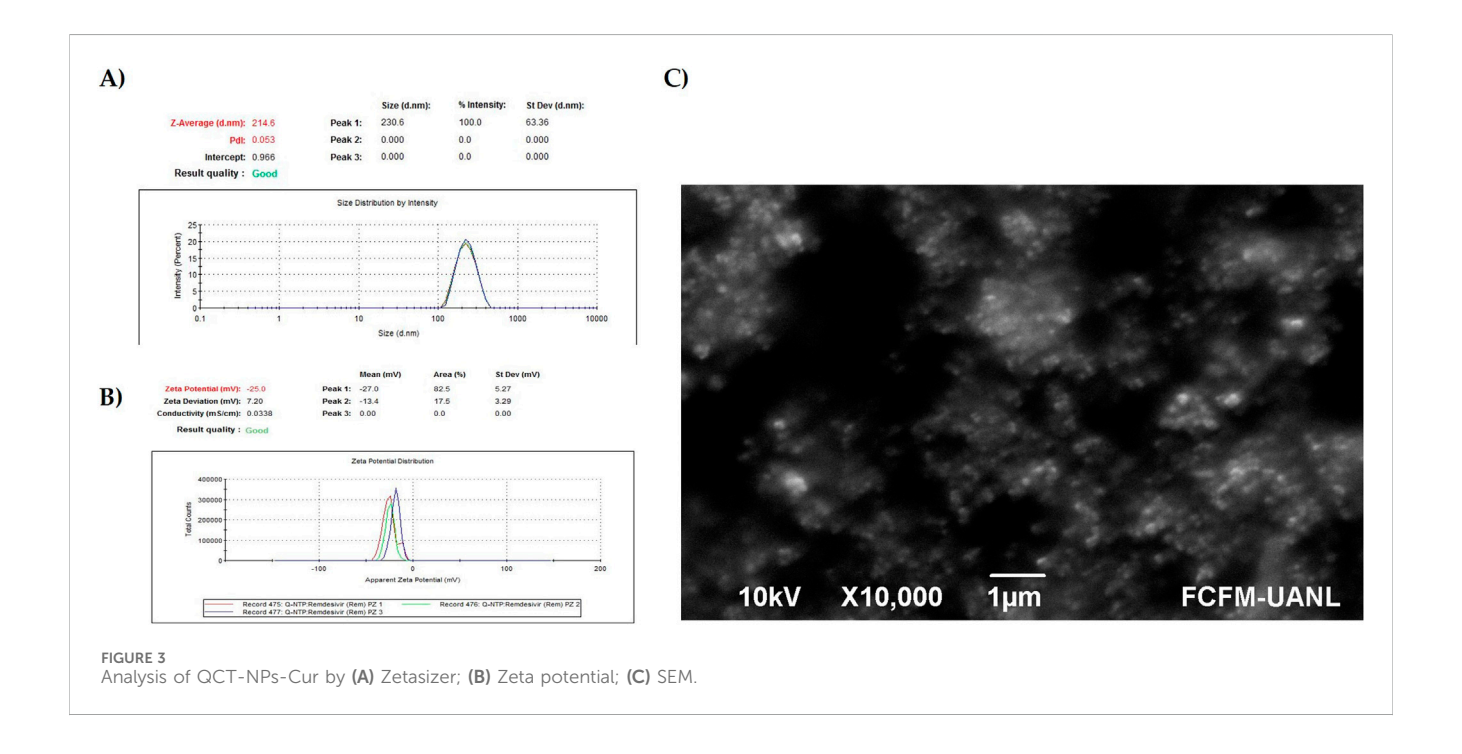
3.2 Determination of drugs (Rem and Cur) encapsulation and release in QCT-NPs

We obtained an encapsulation efficiency of 91.51% with remdesivir in the QCT-NPs + Rem according to the formula % EE = [(Drug added - Free "unentrapped drug")/Drug added] *100.

In the case of curcumin, we obtained an encapsulation efficiency of 86.40% in the QCT-NPs + Cur. Figure 5A) corresponds to the percentage of Rem and Cur released in the QCT-NPs + Rem and QCT-NPs-Cur. The drugs were progressively released until reaching a high level of release at 48 h and almost total release at 72 h.







According to zero-order drug release kinetics, a drug is released from a drug delivery system at a constant rate per unit of time, independent of concentration. To evaluate the drug release by zero-order kinetics, a graph was plotted between time and cumulative drug release % (Figure 5B). The slope of the graph provides a rate constant for the zero-order model. The correlation

coefficient R^2 can be used to predict whether the drug release follows a zero-order model (Jayachandran P. et al., 2023).

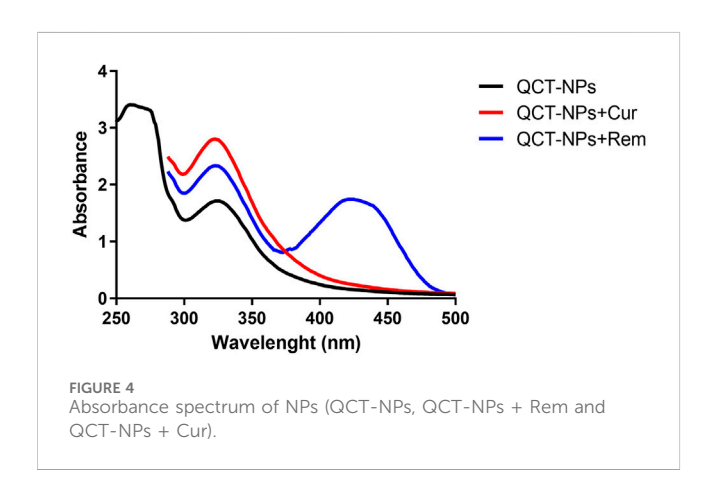
These results suggest that both formulations exhibit approximately zero-order release behavior in the 0–24 h range, with *Free Cur* showing a slightly higher release rate and better linearity ($R^2 = 0.93$) than *Free Rem* ($R^2 = 0.89$). This indicates a more

TABLE 1 Physicochemical parameters obtained from the characterization of the quercetin-based nanoparticles.

Property	QCT-NPs	QCT-NPs + Rem	QCT-NPs + Cur
Size (DLS, nm)	209.0 ± 21.8 199.2		214.6
Zeta potential (mV)	-34.7	-25.0	-19.0
Morphology (AFM)	Spherical Spherical		Spherical
Stability	Stable at 4 °C and 20 °C. Unstable at RT	Stable at 4 °C and 20 °C. Unstable at RT	Stable at 4 °C and 20 °C. Unstable at RT
Encapsulation (EE%)	-	91.5%	86.4%
Drug release	-	Sustained (72 h)	Sustained (72 h)
Cytotoxicity (viability in Vero E6, IC50)	75.8% (18.20 μM)	82.5%	78.0%

TABLE 2 Stability of QCT-NPs, QCT-NPs-Rem and QCT-NPs-Cur at RT, 4 °C, and -20 °C.

Formulation	Parameter	4 °C	RT (room temperature)	–20 °C
QCT-NPs	Size (nm)	214.8	72.32	214.52
	Z potential (mV)	-24.00	-32.58	-32.90
QCT-NPs + Rem	Size (nm)	202.12	345.82	201.32
	Z potential	-19.72	-25.34	-25.42
QCT-NPs + Cur	Size (nm)	223.76	335.96	220.70
	Z potential (mV)	-14.72	-21.14	-21.58



consistent and sustained drug release for Free Cur during the initial phase.

3.3 Cytotoxicity in Vero E6 cells induced by QCT-NPs by MTT assay

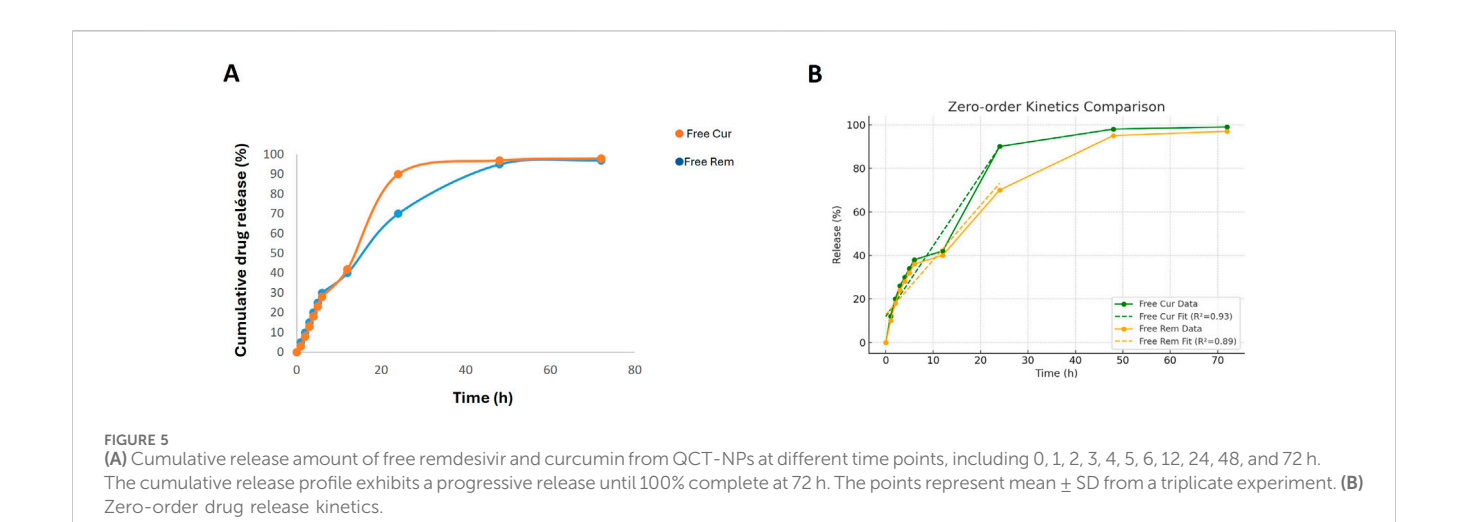
The cytotoxicity of quercetin-based nanoparticles (QCT-NPs) was assessed in Vero E6 cells using the MTT assay. As illustrated in Figure 7A, QCT-NPs demonstrated favorable biocompatibility across a range of concentrations. At the chosen concentration of $18.20~\mu\text{M}$, cell viability remained relatively high at 75.8%. In

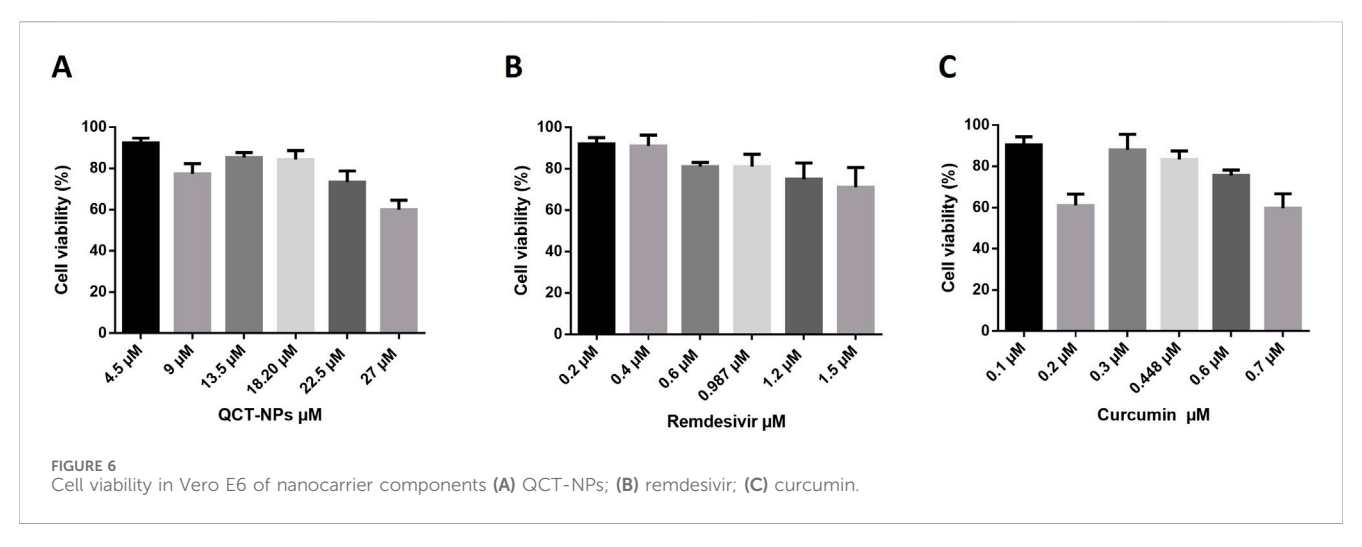
comparison, treatment with remdesivir (Rem) led to a concentration-dependent decrease in cell viability, which reached 82.5% at the concentration of interest (Figure 7B). For curcumin (Cur), the viability of treated cells was 78.0% (Figure 6C), indicating moderate cytocompatibility.

3.4 Evaluation of the antiviral activity of QCT-NPs in pseudovirus neutralization

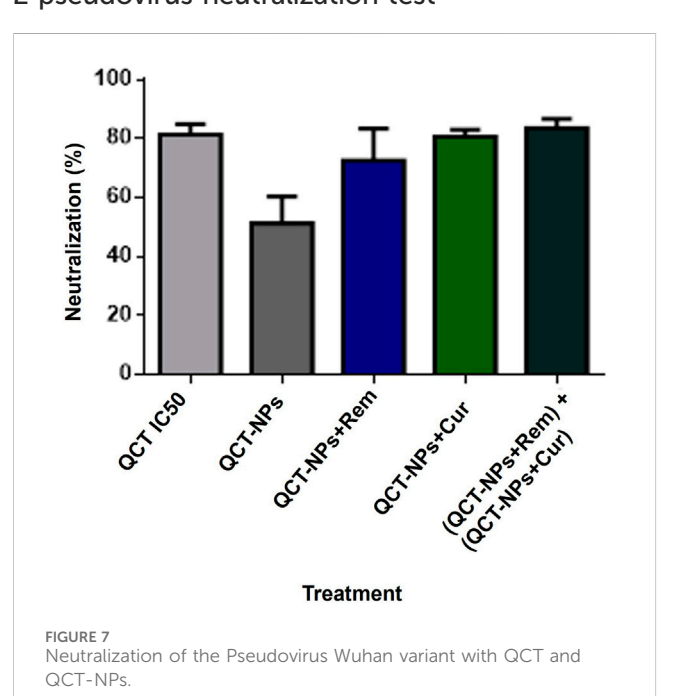
Figure 7 illustrates the percentage of inhibition of the Wuhan strain pseudovirus (rSARS-CoV-2) following treatment with various formulations. Free quercetin demonstrated an inhibition rate of 81.4% at its IC $_{50}$, while QCT-NPs exhibited a lower inhibitory effect of 50%. The QCT-NPs + Rem formulation achieved an inhibition rate of 72.7%, and QCT-NPs + Cur displayed a slightly higher effect at 79.8%. The combined treatment of QCT-NPs-Rem and QCT-NPs + Cur resulted in an inhibition rate of 82.1%, which was not significantly different from the individual treatments.

Figure 8 illustrates the inhibitory effects against the Delta variant pseudovirus. At the IC $_{50}$, quercetin achieved 100% inhibition, while QCT-NPs demonstrated 50% inhibition. In this instance, QCT-NPs-Rem attained 98% inhibition, and QCT-NPs + Cur exhibited 88% inhibition. The combined treatment (QCT-NPs + Rem)+ (QCT-NPs + Cur) sustained a high inhibition rate of 98%, with no significant synergistic enhancement observed over the individual formulations.

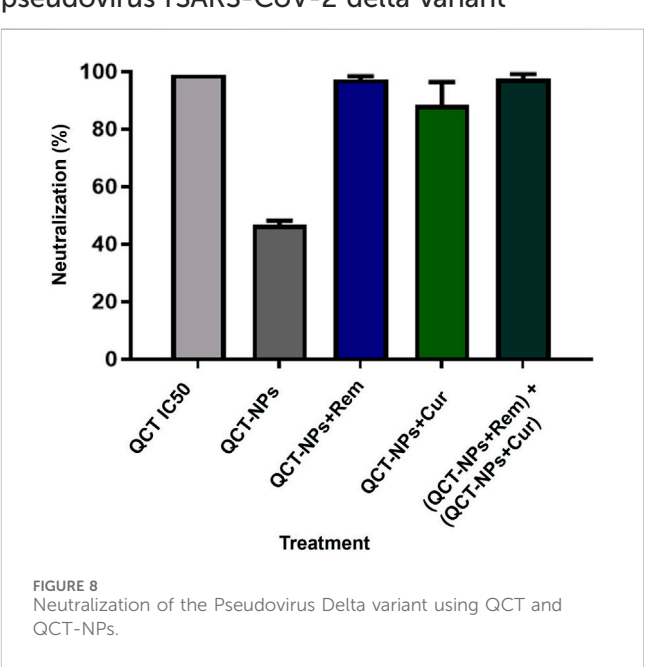




3.4.1 Wuhan recombinant rSARS-CoV-2 pseudovirus neutralization test



3.4.2 Neutralization test of the recombinant pseudovirus rSARS-CoV-2 delta variant



4 Discussion

We synthesized nanoparticles from quercetin as a base (QCT-NPs) through oxidative (self) polymerization. The oxidation of quercetin was achieved in alkaline solutions, where the basic pH promotes the deprotonation of catechol groups, leading to the formation of quercetin quinone (Sunoqrot et al., 2019; Ball V., 2018). The sizes of the QCT-NPs obtained were 209.9 \pm 21.8 nm, with a Polydispersity Index (PDI) value of 0.090 \pm 0.080 (Figure 1A). As previously mentioned, the size of nanoparticles is crucial as it influences the encapsulation, release, and stability of the compound within them. Similar sizes have been reported, ranging from 177.4 to 202.6 nm in diameter, with a PDI value of 0.14 (Souza et al., 2014; Marques, S., and Segundo, M. A., 2024; Öztürk et al., 2024; Sunoqrot et al., 2019).

Under an atomic force microscope (AFM) (Figure 1C), the quercetin nanoparticles exhibit a well-defined spherical shape, measuring approximately 200 nm. However, both agglomerates and aggregates are present in the sample; in all forms, the particles remain well-defined. The sizes of the QCT-NPs + Rem and QCT-NPs + Cur were measured at 208.6 ± 24.4 nm and 200.6 ± 18.5 nm, respectively (Figures 2, 3). The stability of nanoparticles is a crucial characteristic for their effective functioning in targeted delivery systems (Wu et al., 2011; Sultana et al., 2020; Mitchell et al., 2021). Various conditions have been documented that affect quercetin stability, including oxygen concentration, high pH levels, temperature, and storage conditions, all of which negatively impact quercetin degradation (Buchner et al., 2006).

The physicochemical stability of the quercetin-based nanoparticle formulations was assessed for 6 weeks at three storage temperatures: room temperature (RT), 4 $^{\circ}$ C, and -20 $^{\circ}$ C seen in Table 2.

For QCT-NPs, the hydrodynamic size remained relatively stable at 4 $^{\circ}$ C and -20 $^{\circ}$ C; in contrast, a significant decrease in size was observed at RT. The reduction may be attributed to aggregation, partial disintegration, or restructuring of the nanoparticle matrix under ambient conditions. Conversely, potential became more negative at 4 $^{\circ}$ C and RT, indicating increased mV. This change is due to enhanced electrostatic repulsion.

In the case of QCT-NPs + Rem, the particle size significantly increased at room temperature aggregation potential and druginduced destabilization at higher temperatures. Elevated zeta potential was also exhibited across values conditions (-19.72 mV to -25.42 mV).

Similarly, QCT-NPs + Cur exhibited a comparable pattern, with particle size increasing significantly at RT (335.96 nm) compared to cold storage conditions (~220 nm). The zeta potential values remained less negative overall (-14.72 to -21.58 mV), indicating that curcumin loading may reduce the net surface charge, potentially due to hydrophobic interactions or partial shielding of surface functional groups.

It has been proven that negatively charged nanoparticles can interact with and even inhibit the virus because, although the overall surface of SARS-COV-2 is slightly negative, it is not uniform since the receptor-binding domain (RBD) of the Spike protein has positively charged localized regions, particularly in variants such as Delta and Omicron (Božič and Podgornik, 2023). These regions could interact with our nanoparticles. Additionally, there are hydrophobic interactions, hydrogen bonds, and van der Waals forces that can

stabilize the nanoparticle-virus complex even if there is net charge repulsion. The cell membrane has a negative charge because it contains glycoproteins and phospholipids, allowing interaction with negatively charged nanoparticles through endocytic pathways such as pinocytosis or receptor-mediated endocytosis (Rennick J et al., 2021). Negatively charged nanoparticles have been shown to have lower cytotoxicity and reduced opsonization, which represents an advantage for improving their biocompatibility and stability *in vivo* (Zhang et al., 2011).

These results indicate that cold storage (4 °C or –20 °C) preserves the structural integrity and surface charge of the nanoparticle formulations, particularly for drug-loaded systems. In contrast, RT conditions may compromise colloidal stability, especially in formulations coloaded with remdesivir or curcumin, likely due to temperature-induced aggregation or alterations in drug-polymer interactions (Perrett J et al., 2016; Rachmawati H et al., 2016).

The release of drugs from polymeric nanocarriers typically exhibits a biphasic profile, consisting of an initial phase characterized by a rapid release, followed by a second phase of sustained release. The accelerated release is often attributed to the dissociation of molecules bound to the surface, while the sustained release is associated with the slow diffusion of more tightly bound and/or encapsulated molecules (Ding et al., 2017; Son et al., 2017; Kwon and Kataoka, 2012). The results indicate that both remdesivir and curcumin demonstrate sustained release (see Figures 5A,B). Sunoqrot et al. (2019) note that this phenomenon occurs due to the high affinity of remdesivir and curcumin for QCT-NPs, suggesting that stable and effective nanoparticles have been produced for administration in both *in vitro* and *in vivo* settings.

The cell viability results we obtained are above 70%, and the concentrations we use are based on the IC50 values applied in the neutralization tests. In Figure 6A, the viability of QCT-NPs μM obtained a 79%, while the value of remdesivir was achieved at 82% (Figure 7B). The IC50 of Cur was 0.448 μM and reached 79% of viability. As noted, the concentrations used for pseudovirus inhibition tests do not represent significant toxicity.

The cytotoxicity profiles of quercetin-based nanoparticles (QCT-NPs), remdesivir (Rem), and curcumin (Cur) were evaluated in Vero E6 cells across a range of concentrations (Figure 6). All treatments preserved acceptable levels of cell viability (>70%) at the tested concentrations, indicating low inherent cytotoxicity and good biocompatibility.

QCT-NPs (Figure 6A) exhibited minimal cytotoxicity, with cell viability consistently exceeding 75%, even at elevated concentrations. These findings are consistent with those of previous studies indicating that quercetin, when encapsulated in biocompatible nanocarriers, demonstrates reduced cytotoxicity due to controlled release and improved cellular uptake (Liu et al., 2021; Javani et al., 2021). The negative surface charge and nanoscale dimensions of QCT-NPs may also enhance stability and decrease nonspecific cellular interactions (Kakran et al., 2012).

Remdesivir-treated cells, although clinically approved for antiviral therapy, demonstrated a modest reduction in cell viability with increasing concentrations, reaching approximately 82.5% at the tested doses (Figure 6B). This finding is consistent with those of previous *in vitro* studies that reported dose-dependent cytotoxicity of remdesivir in Vero and human epithelial cell lines (Pruijssers et al., 2020).

Curcumin-treated cells demonstrated a viability of approximately 78%, indicating moderate cytocompatibility

(Figure 6C). Curcumin is widely acknowledged for its favorable safety profile; however, its solubility and susceptibility to oxidative degradation can impact its biological efficacy. When incorporated into nanoparticulate systems, its cytotoxicity generally decreases due to enhanced protection from degradation and improved delivery (Yallapu et al., 2012; Wang et al., 2023).

In the neutralization assay of the pseudovirus rSARS-CoV-2 (Figures 7, 8), the results indicated that the IC50 of quercetin demonstrated an 81.3% neutralization effect against the Wuhan variant and a 99.08% neutralization effect against the Delta variant. It is hypothesized that the enhanced neutralization of the pseudovirus in the Delta variant is attributable to the action of quercetin, potentially linked to the specific mutation that characterizes the Delta variant: P68IR. This mutation involves the substitution of a proline (Pro) residue with an arginine (Arg) residue, which occurs in the spike protein region known as the "furin cleavage site" (Liu et al., 2021; Xiao Z et al., 2023). This is responsible for making a cut in the S protein, triggering emerging viral particles to be infectious from the moment they leave the host cell (Callaway, 2021). The mutation will likely lead to a conformational change that allows both the molecule and the quercetin nanoparticle to have more affinity to bind to the S protein, inhibiting binding to ACE-2 since the tertiary structure of the amino acids SER349, LEU441, and ASN450, which are known to interact with quercetin, is located close to it (Saakre, et al., 2021). Quercetin has multiple roles within the synergy of the interaction with SARS-CoV-2 (Agrawal, P K et al., 2020; Gasmi A et al., 2022; Pan et al., 2023). Abian et al. (2020) showed that quercetin has the ability to inactivate the 3C-like protease of SARS-CoV-2 (3CLpro). It is also suspected that it also possesses ionophoric properties of zinc, especially since zinc inhibits SARS-CoV-2 RNA-dependent RNA polymerase activity (Pawar and Pal, 2020; Pormohammad A et al., 2021). As we could already appreciate, quercetin has a double role as a carrier of drugs as well as an adjuvant in viral inhibition.

As previously mentioned, remdesivir is antiviral drug approved by the U.S. Food and Drug Administration (FDA) for the treatment of COVID-19 (Godwin P.O et al., 2023; Patrick-Brown et al., 2024). In light of the ongoing global efforts to identify alternative or adjunct therapies to combat SARS-CoV-2 infection, the development of nanocarrier-based systems, such as quercetin-loaded nanoparticles (QCT-NPs), has garnered increasing attention.

In this study, QCT-NPs exhibited consistent antiviral activity against both the Wuhan and Delta pseudovirus variants, achieving inhibition levels near 50% at the IC_{50} . This indicates a stable baseline of neutralization efficacy, which can be attributed to quercetin's established ability to disrupt viral entry and replication pathways (Xiao et al., 2023).

The QCT-NPs-Rem formulation demonstrated enhanced neutralization, achieving 72.7% inhibition against the Wuhan variant and a significantly higher 98% inhibition against the Delta variant. This substantial increase may be attributed to the P681R mutation in the spike protein of the Delta variant, which enhances furin-mediated cleavage and facilitates viral entry, potentially increasing susceptibility to the mechanism of action of remdesivir (Liu et al., 2021). Furthermore, the antiviral activity of remdesivir is mediated through the incorporation of its active metabolite GS-443902 (remdesivir triphosphate) into nascent viral RNA, resulting in delayed chain termination after the addition of three nucleotides (Pruijssers et al., 2020).

Curcumin, a natural polyphenol, has also shown moderate neutralization effects. Its incorporation into QCT-NP-Cur formulations underscores the potential of natural molecules in combination with nanotherapeutics. The combined treatment of QCT-NPs-Rem and QCT-NPs-Cur achieved a neutralization rate of 79.8% for the Wuhan variant and 88% for the Delta variant. While these results indicate an additive trend, no statistically significant synergistic effect was observed in this formulation when compared to the individual components. These findings underscore the potential of quercetin- and curcumin-based nanocarriers as complementary antiviral agents, particularly when formulated with drugs such as remdesivir. However, further mechanistic studies and in vivo validations are necessary to explore their therapeutic synergy and pharmacodynamic interactions in greater detail. As a continuation of our *in vitro* findings, we will implement an in vivo pseudovirus-based model (Tseng et al., 2021) to evaluate the efficacy of our therapeutic strategy against SARS-CoV-2 entry.

5 Conclusion

The self-assembly of quercetin into nanoparticle-based carriers facilitates the encapsulation and enhances the solubility of hydrophobic antiviral molecules. Our findings demonstrate that these quercetin-based nanocarriers exhibit significant inhibitory activity against both the Wuhan strain and the Delta variant of the SARS-CoV-2 pseudovirus. These promising results highlight the potential of this nanoplatform as a novel antiviral strategy and support the continuation of this research in preclinical *in vivo* models to further validate its efficacy and translational relevance.

Data availability statement

The raw data supporting the conclusions of this article will be made available by the authors, without undue reservation.

Author contributions

CA-B: Writing - original draft, Writing - review and editing. MD-E: Investigation, Writing - review and editing. LT-A: Writing - original draft, Writing - review and editing. AU-P: Formal Analysis, Writing - review and editing. IL-C: Formal Analysis, Writing - review and editing. AM-R: formal Analysis, Writing editing. MR-R: Methodology, review and Writing review and editing. EP-T: Methodology, Writing - review and editing. RT-G: Resources, Supervision, and editing. CR-P: review Supervision, Writing - review and editing. JM-G: Conceptualization, Supervision, Writing - review and editing.

Funding

The author(s) declare that no financial support was received for the research and/or publication of this article.

Conflict of interest

The authors declare that the research was conducted in the absence of any commercial or financial relationships that could be construed as a potential conflict of interest.

Generative AI statement

The author(s) declare that no Generative AI was used in the creation of this manuscript.

Any alternative text (alt text) provided alongside figures in this article has been generated by Frontiers with the support of artificial

intelligence and reasonable efforts have been made to ensure accuracy, including review by the authors wherever possible. If you identify any issues, please contact us.

Publisher's note

All claims expressed in this article are solely those of the authors and do not necessarily represent those of their affiliated organizations, or those of the publisher, the editors and the reviewers. Any product that may be evaluated in this article, or claim that may be made by its manufacturer, is not guaranteed or endorsed by the publisher.

References

Abian, O., Ortega-Alarcon, D., Jimenez-Alesanco, A., Ceballos-Laita, L., Vega, S., Reyburn, H. T., et al. (2020). Structural stability of SARS-CoV-2 3CLpro and identification of quercetin as an inhibitor by experimental screening. *Int. J. Biol. Macromol.* 164, 1693–1703. doi:10.1016/j.ijbiomac.2020.07.235

Agrawal, P. K., Agrawal, C., and Blunden, G. (2020). Quercetin: antiviral significance and possible COVID-19 integrative considerations. *Nat. Product. Commun.* 15 (12), 1934578X20976293. doi:10.1177/1934578x20976293

Baker, R. E., Mahmud, A. S., Miller, I. F., Rajeev, M., Rasambainarivo, F., Rice, B. L., et al. (2022). Infectious disease in an era of global change. *Nat. Rev. Microbiol.* 20 (4), 193–205. doi:10.1038/s41579-021-00639-z

Ball, V. (2018). Polydopamine nanomaterials: recent advances in synthesis methods and applications. Front. Bioeng. Biotechnol. 6, 109. doi:10.3389/fbioe.2018.00109

Bernardy, A., Höfflin, J., Daum, N., Schneider, M., and Lehr, C. M. (2010). Hydrophilic coating of PLGA nanoparticles with polyvinyl alcohol. Influence on nanoparticle properties and colloidal stability. *J. Nanopart. Res.* 12 (7), 2567–2578. doi:10.1007/s11051-009-9796-1

Božič, A., and Podgornik, R. (2023). Changes in total charge on spike protein of SARS-CoV-2 in emerging lineages. *Bioinforma. Adv.* 4 (1), vbae053. doi:10.1093/bioadv/vbae053

Buchner, N., Krumbein, A., Rohn, S., and Kroh, L. W. (2006). Effect of thermal processing on the flavonols rutin and quercetin. *Rapid Commun. Mass Spectrom.* 20 (21), 3229–3235. doi:10.1002/rcm.2720

Callaway, E. (2021). The mutation that helps Delta spread like wildfire. Nature 596 (7873), 472–473. doi:10.1038/d41586-021-02275-2

Chiu, Y. T., Chiu, C. P., Chien, J. T., Ho, G. H., Yang, J., and Chen, B. H. (2007). Encapsulation of lycopene extract from tomato pulp waste with gelatin and poly (y-glutamic acid) as carrier. *J. Agric. Food Chem.* 55 (13), 5123–5130. doi:10.1021/if0700069

Derosa, G., Maffioli, P., D'Angelo, A., and Di Pierro, F. (2021). A role for quercetin in coronavirus disease 2019 (COVID-19). *Phytotherapy Res.* 35 (3), 1230–1236. doi:10. 1002/ptr.6887

Ding, C., and Li, Z. (2017). A review of drug release mechanisms from nanocarrier systems. *Mater. Sci. Eng. C* 76, 1440–1453. doi:10.1016/j.msec.2017.03.130

Doi, Y., Hibino, M., and Hase, R. (2021). A prospective, randomized, open-label trial of early versus late favipiravir therapy in hospitalized patients with COVID-19. *Antimicrob. Agents Chemother.* 65 (12), e01897–21. doi:10.1128/AAC.01897-21

Gasmi, A., Mujawdiya, P. K., Lysiuk, R., Shanaida, M., Peana, M., Gasmi Benahmed, A., et al. (2022). Quercetin in the prevention and treatment of coronavirus infections: a focus on SARS-CoV-2. *Pharm. (Basel). Aug 25* 15 (9), 1049. doi:10.3390/ph15091049

Godwin, P. O., Oppelt, T. F., and Caron, M. F. (2023). Remdesivir for the treatment of COVID-19: a narrative review. *Infect. Dis. Ther.* 12 (1), 1–16. doi:10.1007/s40121-023-00900-3

Jackman, J. A., Lee, J., and Cho, N. J. (2016). Nanomedicine for infectious disease applications: innovation towards broad-spectrum treatment strategies. *Acta Biomater*. 43, 14–29. doi:10.1016/j.actbio.2016.07.034

Javani, R., Hashemi, F. S., Ghanbarzadeh, B., and Hamishehkar, H. (2021). Quercetin-loaded niosomal nanoparticles prepared by the thin-layer hydration method: formulation development, colloidal stability, and structural properties. *LWT - Food Sci. Technol.* 141, 110865. doi:10.1016/j.lwt.2021.110865

Jayachandran, P., Ilango, S., Suseela, V., Nirmaladevi, R., Shaik, M. R., Khan, M., et al. (2023). Green synthesized silver nanoparticle-loaded Liposome-based Nanoarchitectonics for cancer Management: *in vitro* drug release analysis. *Biomedicines* 11 (1), 217. doi:10.3390/biomedicines11010217

Kakran, M., Shegokar, R., Sahoo, N. G., Al Shaal, L., Li, L., and Müller, R. H. (2012). Fabrication of quercetin nanocrystals: comparison of different methods. *Eur. J. Pharm. Biopharm.* 80 (1), 113–121. doi:10.1016/j.ejpb.2011.08.006

Kandeil, A., Mostafa, A., Göertz, G., Dijkman, R., and Haagmans, B. L. (2021). Quercetin inhibits SARS-CoV-2 replication *in vitro* with an IC $_{50}$ of 18.2 μ M. *Virology J.* 21, 99. doi:10.1186/s12985-024-02299-w

Kumari, A., Yadav, S. K., Pakade, Y. B., Singh, B., and Yadav, S. C. (2010). Development of biodegradable nanoparticles for delivery of quercetin. *Colloids Surfaces B Biointerfaces* 80, 184–192. doi:10.1016/j.colsurfb.2010.06.002

Lipsitch, M., and y Eyal, N. (2017). Improving vaccine trials in infectious disease emergencies. *Science* 357 (6347), 153–156. doi:10.1126/science.aam8334

Liu, Y., Wang, Y., Song, S., Gao, Y., Wang, S., and Wang, S. (2021). Improving physicochemical stability of quercetin-loaded hollow zein particles with chitosan/pectin complex coating. *Antioxidants* 10 (9), 1476. doi:10.3390/antiox10091476

Marques, S. S., and Segundo, M. A. (2024). Nanometrics goes beyond the size: Assessment of nanoparticle concentration and encapsulation efficiency in nanocarriers. *TrAC Trends Anal. Chem.* 174, 117672. doi:10.1016/j.trac.2024.117672

Mitchell, M. J., Billingsley, M. M., Haley, R. M., Wechsler, M. E., Peppas, N. A., and Langer, R. (2021). Engineering precision nanoparticles for drug delivery. *Nat. Rev. Drug Discov.* 20, 101–124. doi:10.1038/s41573-020-0090-8

Nathiya, S., Durga, M., and Devasena, T. (2014). Preparation, physico-chemical characterization and biocompatibility evaluation of quercetin loaded chitosan nanoparticles and its novel potential to ameliorate monocrotophos induced toxicity.

Oliver, S., Hook, J. M., and Boyer, C. (2017). Versatile oligomers and polymers from flavonoids – a new approach to synthesis. *Polym. Chem.* 8 (15), 2317–2326. doi:10.1039/c7py00325k

Öztürk, K., Kaplan, M., and Çalış, S. (2024). Effects of nanoparticle size, shape, and zeta potential on drug delivery. *Int. J. Pharm.* 666, 124799. doi:10.1016/j.ijpharm.2024. 124799

Pan, B., Fang, S., Wang, L., Pan, Z., Li, M., and Liu, L. (2023). Quercetin: a promising drug candidate against the potential SARS-CoV-2-Spike mutants with high viral infectivity. *Comput. Struct. Biotechnol. J.* 21, 5092–5098. doi:10.1016/j.csbj.2023.10.029

Pascual-Figal, D. A., Martínez-González, S., Pérez-Martínez, M. T., and García-García, C. (2022). Multiorgan impact of COVID-19: Pathogenesis and clinical consequences. *Ann. Med.* 54 (1), 341–352. doi:10.1080/07853890.2022.2026871

Patrick-Brown, T. D. J. H., Barratt-Due, A., Trøseid, M., Dyrhol-Riise, A. M., Nezvalova-Henriksen, K., Kåsine, T., et al. (2024). The effects of remdesivir on long-term symptoms in patients hospitalised for COVID-19: a pre-specified exploratory analysis. *Commun. Med.* 4, 231. doi:10.1038/s43856-024-00650-4

Pawar, A., and Pal, A. (2020). Molecular and functional resemblance of dexamethasone and quercetin: a paradigm worth exploring in dexamethasone-nonresponsive COVID-19 patients. *Phytotherapy Res.* 34, 3085–3088. doi:10.1002/ptr.6886

Perrett, J. (2016). Influence of temperature on colloidal stability of polymer-coated gold nanoparticles in biological media. *J. Colloid Interface Sci.* 483, 123–131. doi:10. 1016/j.jcis.2016.08.052

Pizzorno, A., Padey, B., Dubois, J., Julien, T., Traversier, A., Dulière, V., et al. (2020). *In vitro* evaluation of antiviral activity of single and combined repurposable drugs against SARS-CoV-2. *Antivir. Res.* 181, 104878. doi:10.1016/j.antiviral.2020.104878

Pormohammad, A., Monych, N. K., and Turner, R. J. (2021). Zinc and SARS-CoV-2: a molecular modeling study of Zn interactions with RNA-dependent RNA-polymerase and 3C-like proteinase enzymes. *Int. J. Mol. Med.* 47 (1), 326–334. doi:10.3892/ijmm. 2020.4790

Pruijssers, A. J., George, A. S., Schäfer, A., Leist, S. R., Gralinksi, L. E., Dinnon III, K. H., et al. (2020). Remdesivir inhibits SARS-CoV-2 in human lung cells and chimeric SARS-CoV expressing the SARS-CoV-2 RNA polymerase in mice. *Cell Rep.* 32 (3), 107940. doi:10.1016/j.celrep.2020.107940

Rachmawati, H., Rahma, A., Al Shaal, L., Müller, R. H., and Keck, C. M. (2016). Destabilization mechanism of ionic Surfactant on curcumin Nanocrystal against Electrolytes. *Sci. Pharm.* 84 (4), 685–693. doi:10.3390/scipharm84040685

Rennick, J. J., Johnston, A. P. R., and Parton, R. G. (2021). Key principles and methods for studying the endocytosis of biological and nanoparticle therapeutics. *Key Princ. methods Stud. endocytosis Biol. nanoparticle Ther. Nat. Nanotechnol.* 16 (3), 266–276. doi:10.1038/s41565-021-00858-8

Saakre, M., Mathew, D., and Ravisankar, V. (2021). Perspectives on plant flavonoid quercetin-based drugs for novel SARS-CoV-2. *Beni-Suef Univ. J. Basic Appl. Sci.* 10 (1), 21–13. doi:10.1186/s43088-021-00107-w

Son, G. H., Lee, B. J., and Cho, C. W. (2017). Mechanisms of drug release from advanced drug formulations such as polymeric-based drug-delivery systems and lipid nanoparticles. *J. Pharm. Investigation* 47, 287–296. doi:10.1007/s40005-017-0320-1

Souza, M. P., Vaz, A. F., Correia, M. T., Cerqueira, M. A., Vicente, A. A., and Carneiro-da-Cunha, M. G. (2014). Quercetin-loaded lecithin/chitosan nanoparticles for functional food applications. *Food bioprocess Technol.* 7 (4), 1149–1159. doi:10.1007/s11947-013-1160-2

Sultana, S., Alzahrani, N., Alzahrani, R., Alshamrani, W., Aloufi, W., Ali, A., et al. (2020). Stability issues and approaches to stabilised nanoparticles based drug delivery system. *J. Drug Target* 28 (5), 468–486. doi:10.1080/1061186X.2020.1722137

Sunoqrot, S., Al-Shalabi, E., Hasan Ibrahim, L., and Zalloum, H. (2019). Nature-inspired polymerization of quercetin to produce antioxidant nanoparticles with controlled size and skin tone-matching colors. *Molecules* 24 (21), 3815. doi:10.3390/molecules24213815

Tao, K., Tzou, P. L., Kosakovsky Pond, S. L., Shafer, R. W., Ostergaard, S. D., Morgan, C. N., et al. (2021). Teaching a new mouse old tricks: Humanized mice as an infection

model for Variola virus. PLoS Pathog. 17 (7), e1009633. doi:10.1371/journal.ppat. 1009633

Tseng, S. H., Lam, B., Kung, Y. J., Lin, J., Liu, L., Tsai, Y. C., et al. (2021). A novel pseudovirus-based mouse model of SARS-CoV-2 infection to test COVID-19 interventions. *J. Biomed. Sci.* 28, 34. doi:10.1186/s12929-021-00729-3

Uliasz, T. F., and Hewett, S. J. (2000). A microtiter trypan blue absorbance assay for the quantitative determination of excitotoxic neuronal injury in cell culture. *J. Neurosci. Methods* 100 (1-2), 157-163. doi:10.1016/s0165-0270(00)00248-x

Ulmer, J. B., and Valley, U. y. R. R. (2006). Vaccine manufacturing: challenges and solutions. *Nat. Biotechnol.* 24 (11), 1377–1383. doi:10.1038/nbt1261

Wu, Z., and McGoogan, J. M. (2020). Characteristics of and important lessons from the coronavirus disease 2019 (COVID-19) outbreak in China: Summary of a report of 72,314 cases from the Chinese Center for Disease Control and Prevention. *JAMA* 323 (13), 1239–1242. doi:10.1001/jama.2020.2648

Wu, L., Zhang, J., and Watanabe, W. (2011). Physical and chemical stability of drug nanoparticles. Adv. drug Deliv. Rev. 63 (6), 456–469. doi:10.1016/j.addr.2011.02.001

Xiao, Z., Xu, J., Zhou, X., Li, J., Zhang, H., and Chen, Z. (2023). Quercetin effectively inhibits SARS-CoV-2 and its variants in pseudovirus-based neutralization assays. *J. Nat. Prod. Res.* 12 (3), 205–213. doi:10.1016/j.jnpr.2023.01.005

Yallapu, M. M., Jaggi, M., and Chauhan, S. C. (2012). Curcumin nanoformulations: a future nanomedicine for cancer. *Drug Discov. Today* 17 (1-2), 71–80. doi:10.1016/j. drudis.2011.09.009

Zhang, T., Chen, X., Qu, L., Wu, J., Cui, R., Zhao, Y., et al. (2011). Design and evaluation of a self-nanoemulsifying drug delivery system of quercetin. *Int. J. Pharm.* 404 (1–2), 158–168. doi:10.1016/j.ijpharm.2010.11.022

Zhou, J., Krishnan, N., Jiang, Y., Fang, R. H., and y Zhang, L. (2021). Nanotechnology for virus treatment. *Nano Today* 36, 101031. doi:10.1016/j.nantod.2020.101031